Construction of periodic micro-/nanostructures by glancing angle deposition

L. X. HU, P. WANG, X. Y. WAN, S. H. CHEN, S. J. JIANG*
State Key Laboratory of Optoelectronic Materials and Technologies,Sun Yat-sen University, Guangzhou 510275, China

Sculptured thin films (STFs) are a kind of anisotropic thin films with micro-nano structures prepared by glancing angle deposition (GLAD) technique. They exhibit novel optical functional properties. The periodic pre-defined seed layers (PDSLs) introduced to the GLAD process can act as a 'foundation footings' to define the upper structures. In this paper, the relations between structure parameters of PDSLs and experimental deposition parameters are summarized. PDSLs prepared by three different methods are used as substrates for STFs deposition, so that the porous and structure characteristics of STFs can be controlled in three-dimensions and then an effective way for fabricating functional micro/nano devices can be provided.

1. Introduction

Micro/Nano optoelectronic devices have important research and application values in information industry, photo-energy application, and biomedicine etc. Nowadays, as scientific industry gradually becomes the pillar industry of modern economy, how to produce massive high-precision and low-cost micro/nano devices with certain function is a research focus. According to early researches, when thin films are prepared by physical vapor deposition, their density is greatly affected by the vapor deposition angle. When the angle is over 70°, thin films present a porous structure [1]. In 1966, a report in *Nature* [2] by Kevin Robbie et al brought GLAD technique to researchers' attention and ascertained that thin films made by GLAD called STFs, which have provided us with prototypes of micro/nano optoelectronic devices.

STFs in bare substrates show obvious random location. As GLAD is taken as a new kind of technique to produce nano structure, deposition of periodically-located nano-columnar structure becomes the focus of the worldwide researchers. Frequently-used techniques for three-dimensional photonic crystal (PC) fabrication cannot be controlled easily due to their complicated processes. While GLAD is effective and controllable so that fabrication can be realized through regulating fabrication parameters in a single step. Ovidiu Toader et al [3] first proposed this technique in *Science* to fabricate square spiral PC; later M.O. Jensen [4] et al realized it. Other kinds of structures [7-9] such as periodic spiral structures present photonic band gap (PBG) to select circularly polarized light [5]. In addition, introduction of defects into periodic STFs is another key to further utilization of the device [6], which can produce localized defect mode and select the electromagnetic field.

Pre-definition of substrate is the first measure in the fabrication of periodic structures through GLAD. Seed width, seed spacing and structure of PDSL are the main factors that affect the later deposition of Periodic STFs. At present, reported pre-definition techniques include holographic lithography (HL) [10], electron beam lithography (EBL) [11], nanospheres lithography[12]and colloidal self-assembly[13] , etc.

In this paper, we focus on the fabrication of periodic STFs on PDSLs fabricated by three methods: nano-imprint lithography (NIL), HL and EBL. We present the relation between parameters of PDSLs and deposition parameters relying on the theoretical calculations and experiments. We find that HL substrates and NIL substrates are preferable to realize repetitious large-size fabrication. Finally, we draw a comparison of STFs coated in HL substrates with tetragonal periodic pillar or pore arrays and with line defects, and discuss their practical values.

2. Theoretical design of PDSL

The parameters of PDSL have direct impacts on the preparation quality of periodic STFs. Several important principles should be followed to select the proper PDSL [14]: a. the seed spacing should be appropriate to ensure an obvious shadow effect; b. the fill factor of PDSL should match that of the GLAD film in order to make a single thin film column grow on one seed; c. the seed top surface shall be flat and the sidewalls vertical so that it will prevent unintended film growth between seeds.

Fig. 1 (a), (b), (c) and (d) are PDSLs of tetragonal periodic pillar arrays, tetragonal periodic pore arrays, triangle periodic pillar arrays, hexagonal periodic pillar arrays respectively. The s represents the maximum spacing between two adjacent unit cells, d represents seed width, Δ is the period, and h is the height. Fig. 1 (e) and 1(f) are side views. α is the angle of incident flow while γ is the sidewall inclination angle of PDSLs.
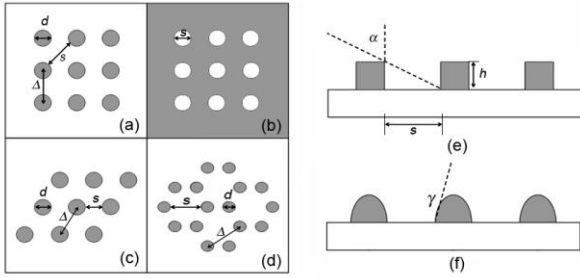

Fig. 1. The structures of PDSLs and the Parameters (a) tetragonal periodic pillar arrays; (b) tetragonal periodic pore arrays; (c) triangle periodic pillar arrays; (d) hexagonal periodic pillar arrays; (e) Side view of ideal sharply defined seeds with a vertical sidewalls and flat top surface; (f) Side view of a more realistic round seed profile with a sidewall inclination angle less than 90°.

A key point in the use of PDSL for GLAD is to ensure that the thin films could grow only on the seeds instead of the gap among them. Therefore, the seed of PDSL should be placed within the shadow of the neighbor seed so that the incident flow can fall on the top surface of it. So the s should match the following formula:

$$s \leq \tan(\alpha) \cdot h \qquad (1)$$

The seed width must approximate to the column diameter so as to keep the periodicity. Therefore, the planar fill factor of the PDSLs $ff_{A,seeds}$ must equal to the volume fill factor of the GLAD thin films $ff_{V,GLAD}$:

$$ff_{A,seeds} = ff_{V,GLAD} \geq \frac{\rho_{GLAD}}{\rho_{bulk}} \qquad (2)$$

In the above inequality, $ff_{V,GLAD}$ is defined as the ratio of a unit volume of the GLAD film to the whole volume of the periodic unit. It approximates to the ratio of the density of GLAD thin film ρ_{GLAD} to the original density of the thin film materials ρ_{bulk}. While $ff_{A,seeds}$ is regarded as the ratio of a seed lattice unit cell that is covered by actual seed material to the area of the lattice unit A. When the lattice unit cell is round, it can be drawn as:

$$ff_{A,seeds} = \frac{\pi d^2}{4} / A \qquad (3)$$

The density of GLAD thin film ρ_{GLAD} as a function of the deposition angle α can be figured out below [15]:

$$\frac{\rho_{GLAD}}{\rho_{bulk}} = \frac{2\cos(\alpha)}{1+\cos(\alpha)} \qquad (4)$$

Putting eq. (3) and eq. (4) into eq. (2), we can get the following formula:

$$\frac{\pi d^2}{4} / A \geq \frac{2\cos(\alpha)}{1+\cos(\alpha)} \qquad (5)$$

In fact, the actual production of the PDSL isn't as ideal as Fig. 1(e). For rounded seeds with sidewall inclination angles below 90°, as shown in Fig. 1 (f), film growth on the sloped sides leads to column broadening and sometimes even complete loss of film periodicity. In practice The seed profile is difficult to control, but experiments with different seed shapes have shown that one should aim for angle higher than 60°[14].

3. Experimental details

The PDSLs used in the experiments include HL substrates, NIL substrates, and EBL substrates.

HL bases on the interference pattern of multiple coherent laser beams to 'carved' a photoresist into periodic microstructures. The patterns depend on the combinations of the superimposing beams (including the angle between the beams) and the laser wavelength [16]. NIL creates patterns by mechanical deformation of imprint resist and subsequent processes. The polymer is coated on the surface of the substrate and the mold board was pressed onto the polymer [17]. EBL generates patterns on a surface through the use of a direct focusing high-voltage electron beam.
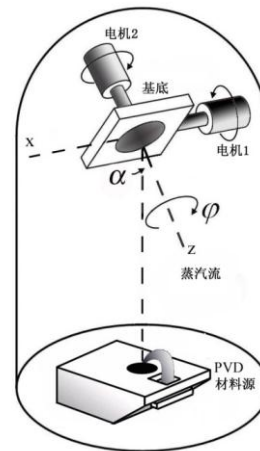

Fig. 2. GLAD apparatus as it is typically implemented in a standard PVD system. Two independent motors accomplish substrate movement.

Several periodic micro-nano thin films were fabricated by GLAD technique on PDSL. Careful selection of the deposition angle (α) and the rotation angle (φ) enables films to possess interesting structural and optical properties [7, 9, 15]. These films were deposited by the use of electron-beam evaporation in a vacuum system with a base pressure of 5×10^{-3} Pa. The materials were pre-evaporated with a lower power of e-beam prior to the deposition. The source purity was 99% or better for all of the materials used. The deposition angle varied from $\alpha = 68°$ to $\alpha = 83°$ for all depositions, and was held constant during each deposition.

If the deposition angle α is held constant, and the substrate is slowly and continuously rotated, the columns will be sculpted into helical columns. As the angular velocity of the substrate rotation is increased, the pitch of the helical structure will approach the diameter of the column. When this occurs, the helical geometry is lost and the structure degenerates into vertical columns. Swing rotation method can be described as follow [14]: During a 'swing' rotation, the substrate is rotated azimuthally back-and-forth within an angular range called the swing angle with a fixed rotation speed. At the end of the deposition of each arm, the substrate was turned through 90° to start the deposition of the next arm. Thus, four adjacent arms make one complete turn of a nano-spiral.

Samples were exposed in a Quanta 400F thermal field emission environmental scanning electron microscope. This instrument was used to obtain top down and cross-sectional images of structures.

4. Results and discussions

4.1 STFs on Various Submicro-scale Periodic Substrates

PDSLs prepared by NIL, HL and EBL technology are shown in Fig. 3(a), 3(c) and 3(e) respectively. These three structures correspond to Fig. 1(a), 1(c) and 1(d).

Table 1 suggests that the less the fill factor of PDSL is, the larger the needed deposited angles become.

Fig. 3(b), 3(d) and 3(f) are top views of thin films. The vertical columnar films were coated on corresponding PDSL at theoretical calculated deposition angle with rotation rate $\omega = 30$r/min. When the period is within submicron scale, top views of thin films coated on different PDSLs are periodic and without bifurcations, which supports the theoretical design. Besides, EBL structure has ideal sharply defined seeds with a vertical sidewalls and flat top surface shown in Fig. 3(e), and corresponding films shown in Fig. 3(f) is rather regular. While NIL substrate shown in Fig. 3(a) and HL substrate shown in Fig. 3(c) exist round seeds with a sidewall inclination angle $60° < \gamma < 90°$. The corresponding coating shown in Fig. 3 (b), (d) is not as regular as Fig. 3

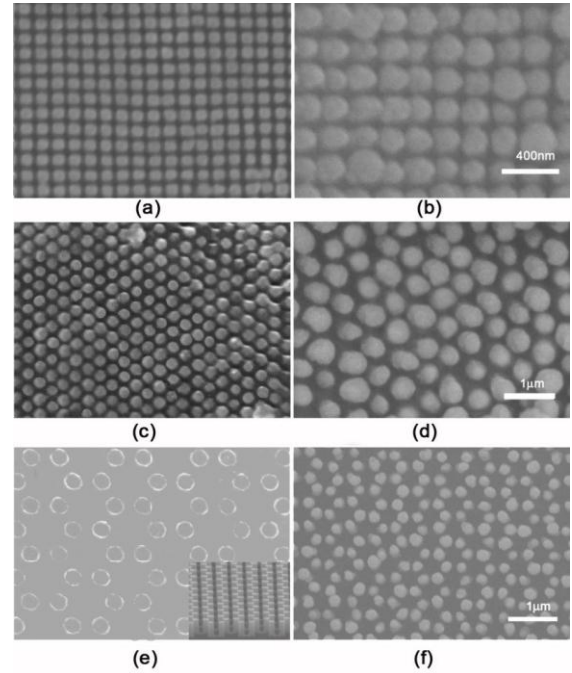(f), but all of them show periodicity.

Fig. 3. Substrate and corresponding periodic thin films (a) NIL substrate; (c) HL substrate; (e) EBL substrate; (b), (d), (f) STFs on corresponding substrate.

Table 1. Substrate structure parameters and corresponding deposited angles.

	Δ (nm)	s (nm)	h (nm)	d (nm)	$ff_{A,seeds}$	α (°)
3(a)	200	140	150	140	0.38	77
3(c)	400	150	200	250	0.35	78
3(e)	500	400	500	190	0.25	83

EBL is low efficiency and high cost, and NIL costs less in mess production, however, once to adjust the size, it needs to adopt EBL to reproduce the template, which costs a lot for the frequent parameter adjustment in experience. Compared with the others, HL only needs to adjust the angle between the beams or the laser wavelength to change periodic size, which is a more effective and low-cost choice to produce large-scale periodic structures.

4.2 STFs on Micro-scale Periodic HL Substrate

STFs were deposited on HL substrates with 1 µm tetragonal periodic pillar or pore arrays shown in Fig. 4(a), 4(c) respectively. When the seed width is wider than the column diameter and the sidewall inclination angle γ is relatively small, it is difficult to grow ideal STFs without bifurcation. All parts of Fig. 4 show "packing" effect in various structures.
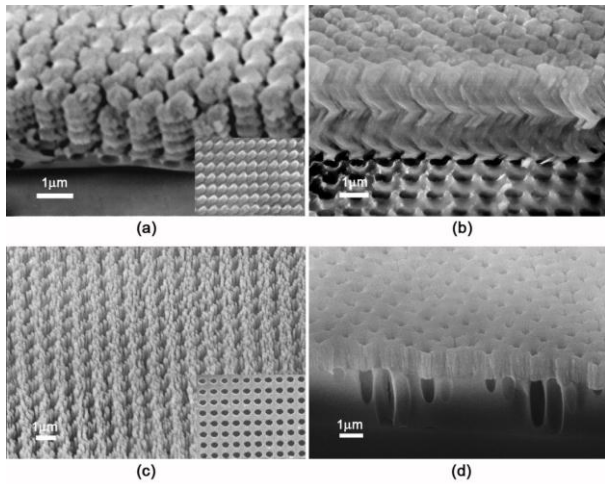
Fig. 4. STFs on HL substrates (a) helical STFs on tetragonal periodic pillar arrays (in the bottom right corner); (b) square spiral STFs on tetragonal periodic pillar arrays; (c) two-level pore STFs thin on tetragonal periodic pore arrays (in the bottom right corner); (d) one-level pore STFs on tetragonal periodic pore arrays.

The helical STFs are available when deposition angle α is held constant at 77° while substrate is rotated continuously with rotation rate $\omega = 0.3r/min$ and deposition rate $r = 1.7nm/s$. The pitch of the helix is 340nm as depicted in Fig. 4(a). The thin films show periodicity in all the three dimensions, in which the period of xy-dimensions could be changed through setting the period of PDSL, and helical period of z axis could be adjusted by the ratio between deposited rate r and rotation rate ω in the following formula:

$$P \approx r/\omega \qquad (6)$$

The square spiral STFs are deposited through swing rotation method, with swing angle within 60°, deposition angle $\alpha = 77°$ and rotation rate $\omega = 0.3r/min$, every 10 swing period turned through 90° to start the deposition of the next arm. The resulting 8 adjacent arms make 2 complete turn of a nano-spiral shown in Fig. 4(b). In the figure, "packing" effect is more obvious than that in Fig. 4(a). The main reason is that the sidewall inclination angle γ is smaller so that some films grow on the sloped sides.

Due to the large-scale of PDSLs and the connection of each periodic unit, the rule of STFs deposition on pore arrays structure is similar to that on bare substrate, exiting irregular column growth. However, because of the existence of periodic pores, novel features of this structure can be dug out.

The vertical columnar STFs are produced by high-speed substrate rotation with rotation rate $\omega = 0.3r/min$ and deposition angle $\alpha = 78°$. The STFs shown in Fig. 4(c) presents two-level pore structure. The 1μm periodic pores are 350 nm wide and are surrounded by

STFs nano-rods. The nano-rods are themselves separated by 5–60 nm gaps, resulting in a two-level pore structure consisting of microscopic and nano-scale pores, 350 and 5–60 nm wide, respectively. The scale of microscopic pores can be adjusted through setting the size of PDSL while fill factor of the nano-rods is decided by deposition angles describe in formula (4). This structure may be ideal for both sensing and catalytic device applications because nano-scale pores maximize the surface area and therefore the reaction site density, while microscopic pores facilitate efficient gas and liquid transport through the functional layer [19].

The STFs present one-level microscopic pore structure is shown in Fig. 4(d). The deposition angle is set as $\alpha = 68°$ in order to make it smaller than the smallest angle (70°) that creates separating column. Compared with Fig. 4(c), it can be noticed that nano-scale pores disappear. The refractive index of STFs can be tuned through choosing different kinds of material and adjusting the deposition angle. When high and low refractive index dielectric materials are alternately deposited and defect layer is introduced, a multilayer stack can produce a narrow transmission notch in the center of a wide stop band, which can be used as narrowband filter [20].

4.3. STFs on Micro-scale Periodic HL Substrate with Line Defect

When defect is introduced into PC to destroy the periodic structure, waveguiding mode within the PBG will emerge. By adjusting the frequency of PBG and waveguiding mode, we can flexibly control the photon [21].
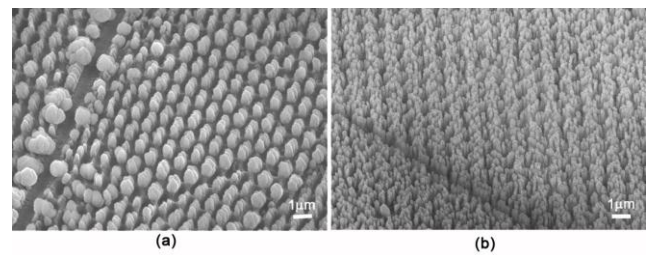

Fig. 5. STFs on HL substrate with line defect (a) tetragonal periodic pillar arrays; (b) tetragonal periodic pore arrays

When the PDSL has defect, STFs can also replicate the defect. The 1 m-period HL substrates exist several hundred micrometers line defects. Fig. 5(a) represents vertical columnar STFs on tetragonal periodic pore arrays substrate. The defect influences the seed sides of PDSL. Some deposition particles gather at the seed side and gain more material in competitive growth. As a result, the columns become wider and present a "packing" effect.

Two-level pore structure with line defect is shown in Fig. 5(b).

5. Conclusions

We have shown how periodic STFs can be fabricated by GLAD on various substrates patterned with PDSLs. According to theoretical designs, parameter setting of PDSLs will influence the STFs deposition. Seed spacing should be within shadow length and fill factor of PDSLs and of STFs should be matched. Vertical sidewalls and flat top surface are ideal for STFs deposition. When parameters of STFs are set, optimum deposition angle should be calculated theoretically. HL, NIL and EBL were used to fabricate PDSLs. Vertical columnar STFs were deposited on the above substrates, which are in good accordance with theoretical designs. By comparing the three substrate preparing methods, we find that HL is a better choice due to its high-effect and low-cost. We fabricated various kinds of periodic STFs on HL substrates with pillar/ pore arrays or defects, including helical STFs, square spiral STFs, two-level pore STFs and one-level pore STFs, and revealed the relations between fabrication parameters and film structures. Potential applications include controllable micro/nano optoelectronic functional devices and etc.

References

[1] R. Messier, J. Vac. Sci. Technol. A **4**, 490 (1986).
[2] K. Robbie, M. J. Brett, A. Lakhtakia, Nature **384**, 616 (1996).
[3] T. Ovidiu, J. Sajeev, Science **292**, 1133 (2001).
[4] M. O. Jensen, M. J. Brett, Opt. Exp. **13**, 3348 (2005).
[5] M. Thiel, M. Decker, M. Deubel, Adv. Mater. **19**, 207 (2007).
[6] F. Wang, A. Lakhtakia, Opt. Exp. **13**, 7319 (2005).
[7] T. Ovidiu, J. Sajeev, Phys. Rev. E **66**, 016610 (2002).
[8] T. Karabacak, G. C. Wang, T. M. Lu, J. Vac. Sci. Technol. A **22**, 1778 (2004).
[9] C. M. Zhou, D. Gall, Small **4**, 1351 (2008).
[10] B. Dick, J. C. Sit, M. J. Brett, Nano. Lett. **1**, 67 (2001).
[11] M. Summers, B. Djurfors, M. J. Brett, J. Microlith. Microfab. Microsyst. **4**, 33012 (2005).
[12] C. Patzig, B. Rauschenbach, B. Fuhrmann, H. S. Leipner, J. Appl. Phys. **103**,024313 (2008).
[13] C. M. Zhou, D. Gall, Thin Solid Films **515**, 1223 (2006).
[14] M. O. Jensen, M. J. Brett, IEEE T. Nanotechnol. **4**, 269 (2005).
[15] R. N. Tait, T. Smy, M. J. Brett, Thin Solid Films **226**, 196 (1993).
[16] H. Misawa, T. Kondo, S. Juodkazis, V. Mizeikis, Shigeki Matsuo, Opt. Exp. **14**, 7943 (2006).
[17] S. Y. Chou, P. R. Krayss, W. Zhang, L. J. Guo, L. Zhuang, J. Vac. Sci. Technol. B **15**, 2897 (1997).
[18] D. X. Ye, T. Karabacak, R. C. Picu, T. M. Lu, Nanotechnology **16**, 1717 (2005).
[19] C. M. Zhou, D. Gall, J. Appl. Phys. **103**, 014307 (2008).
[20] A. Mehta, R. C. Rumpf, Z. Roth, E. G. Johnson, Opt. Lett. **31**, 2903 (2006).
[21] S. John, Phys. Today **44**, 32 (1991).

[*]Corresponding author: stsjsj@mail.sysu.edu.cn